

# Deposition of alumina from dimethylaluminum isopropoxide

Benjamin W. Schmidt<sup>a</sup>, Bridget R. Rogers<sup>a,\*</sup>, William J. Sweet III<sup>a</sup>,  
Cameron K. Gren<sup>b</sup>, Timothy P. Hanusa<sup>b</sup>

<sup>a</sup> Department of Chemical and Biomolecular Engineering, Vanderbilt University, Nashville, TN, USA

<sup>b</sup> Department of Chemistry, Vanderbilt University, Nashville, TN, USA

Available online 5 March 2010

## Abstract

Results from an investigation of chemical vapor deposition of aluminum oxide from dimethylaluminum isopropoxide as a function of deposition temperature at a total pressure of 1.5 mTorr are reported. An effective activation energy for this process was determined to be 85 kJ/mol. Deposited films were shown to be oxygen-rich compared to Al<sub>2</sub>O<sub>3</sub>, with higher deposition temperatures resulting in films closer to stoichiometric alumina. Carbon content of the films increased from approximately 1 to 8 at.% at substrate temperatures of 417 and 659 °C, respectively.  
© 2010 Elsevier Ltd. All rights reserved.

**Keywords:** Films; Al<sub>2</sub>O<sub>3</sub>; Spectroscopy

## 1. Introduction

Trimethylaluminum (TMA) and aluminum tri-isopropoxide (AIP) have been used as precursors for the chemical vapor deposition (CVD) of aluminum oxide.<sup>1</sup> Having a relatively high vapor pressure (approximately 90 Torr) at moderate temperatures (60 °C) makes TMA an attractive CVD precursor for aluminum and aluminum-based materials. Trimethylaluminum contains no oxygen, with each aluminum atom bonded to three carbon atoms. TMA therefore needs a secondary oxygen source to produce aluminum oxide. Also, TMA is pyrophoric which makes it unattractive from a safety standpoint. Aluminum tri-isopropoxide is structured such that each aluminum atom is bonded to three oxygen atoms, and therefore does not need a secondary oxygen source to deposit aluminum oxide. AIP, like other metal alkoxides, tends to oligomerize through intramolecular metal–oxygen bridging. Oligomerization makes the AIP more stable than and less volatile than TMA.<sup>2,3</sup> AIP's vapor pressure is less than 1 Torr at 60 °C. Dimethylaluminum isopropoxide (DMAI) incorporates aspects of both TMA and AIP into its structure. The vapor pressure of DMAI is approximately 10 Torr at 60 °C, and is relatively stable. Aluminum atoms in

DMAI are attached to two carbon atoms and one oxygen atom, making the deposition of aluminum oxide without the need of a secondary oxygen source a possibility.

Koh et al. first reported CVD of aluminum oxide films.<sup>4</sup> Since then, aluminum oxide films have been deposited from DMAI via CVD with O<sub>2</sub>,<sup>5</sup> H<sub>2</sub>O,<sup>6</sup> and N<sub>2</sub>O<sup>8</sup>; by DMAI atomic layer deposition (ALD) with H<sub>2</sub>O<sup>9–11</sup>; and by DMAI plasma-enhanced ALD (PE-ALD) in an oxygen plasma.<sup>7</sup>

In this paper we report the DMAI-sourced CVD of aluminum oxide films deposited on Si (100) substrates. We compare resulting film composition and reaction kinetics to films deposited from TMA and AIP.

## 2. Experimental details

### 2.1. Synthesis of DMAI

Dimethylaluminum isopropoxide (DMAI) was prepared following a reported procedure.<sup>8,9</sup> A 100 mL Schlenk flask equipped with a magnetic stir bar was charged with isopropyl alcohol (15.0 mL, 0.196 mol). The alcohol was degassed and cooled to –78 °C using a mixture of dry ice and acetone. Trimethylaluminum (14.373 g, 0.1994 mol) was then slowly added to the alcohol over 30 min. The reaction was allowed to continue for 30 min after gas evolution had ceased. A clear, colorless liquid was produced. The <sup>1</sup>H NMR spectrum (not shown) was consistent with DMAI spectra reported in the literature.<sup>9</sup>

\* Corresponding author at: Department of Chemical and Biomolecular Engineering, Vanderbilt University, VUStation B 351604, Nashville, TN 37235-1604, USA. Tel.: +1 615 343 3269; fax: +1 615 343 7951.

E-mail address: [bridget.rogers@vanderbilt.edu](mailto:bridget.rogers@vanderbilt.edu) (B.R. Rogers).

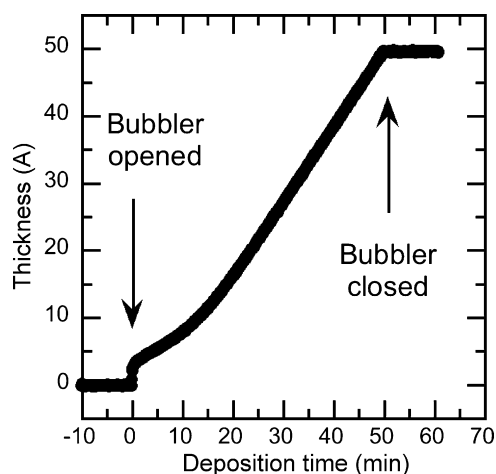


Fig. 1. Representative plot of film thickness versus deposition time as determined by in situ spectroscopic ellipsometry.

## 2.2. CVD process

Films were deposited from DMAI in a high vacuum CVD reactor which has previously been described in detail.<sup>10</sup> Spectroscopic ellipsometry optics (J.A. Woollam M2000-D, Lincoln, NE, USA) were mounted to the chamber behind fused quartz windows at nominally 73° from sample normal.

Substrates temperature during deposition ranged from 417 to 659 °C. Substrate temperature was calibrated to heater set point using a silicon wafer embedded with five thermocouples. DMAI precursor was delivered from a bubbler held at 40 °C using 5 standard cubic centimeters per minute (sccm) of ultrahigh purity nitrogen as the carrier gas. Gas transfer lines between the bubbler and the reactor chamber were maintained at 60 °C to prevent condensation. The total reactor pressure during deposition was approximately 1.5 mTorr, and the DMAI partial pressure was approximately 0.5 mTorr.

Three inch diameter n-type Si (100) substrates were used. H-terminated silicon substrates were prepared by cleaning in a 2 vol.% HF/deionized water (DI) solution for 90 s, rinsing with DI water for 120 s, and blowing dry with nitrogen.<sup>11</sup>

In situ spectroscopic ellipsometry was used to monitor depositions. Substrates were introduced to the reactor and allowed to equilibrate at the desired temperature before the precursor was introduced to the chamber. Fig. 1 is a representative plot of thickness versus deposition time collected during a DMAI CVD process.

## 2.3. Film characterization

Film thickness was determined using spectroscopic ellipsometry (J.A. Woollam M-2000D, Lincoln, NE, USA). Psi and delta values were collected in the photon energy range of 1.2–6.5 eV. A second set of optics was mounted on a tabletop base for *ex situ* ellipsometry analysis. Ellipsometry data were analyzed using software provided by the instrument manufacturer. The optical constants of the prepared substrates were collected prior to deposition, and a Cauchy dispersion layer was used to model the deposited film.

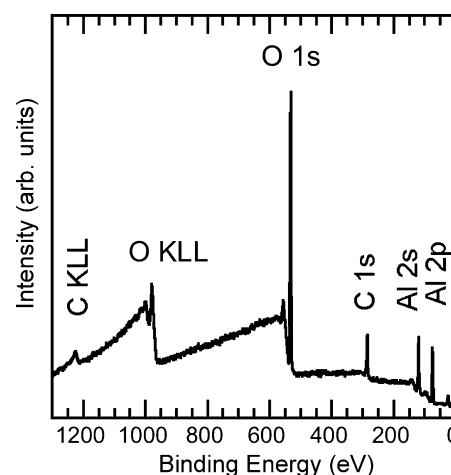


Fig. 2. XPS survey spectrum acquired from a film deposited from dimethylaluminum isopropoxide.

Film elemental composition and bonding were determined using X-ray photoelectron spectroscopy. All analyses were performed on a PHI Versaprobe XPS Microprobe (Physical Electronics, Inc., Chanhassen, MN, USA) using a 50 W monochromatic Al K $\alpha$  X-ray beam (1486.6 eV) and a 200  $\mu$ m spot size. Photoelectrons were collected into a concentric hemispherical analyzer. The analyzer pass energy was 187.85 or 23.50 eV for acquisition of survey or high-resolution spectra, respectively.

## 3. Results and discussion

### 3.1. Film composition

Fig. 2 is the XPS survey scan of a nominal 125 Å thick film deposited at 599 °C. Aluminum, oxygen, and carbon were the only detected elements. Peaks located at approximately 100 and 150 eV binding energies are related to energy-loss phenomena of the Al 2p and Al 2s peaks and not due to the presence of silicon. The thickness of the film analyzed in Fig. 2 was larger than the escape depth of photoelectrons ejected from silicon atoms. Silicon peaks were present in spectra acquired from nominally 50 Å thick films. These silicon peaks were assumed to originate from the silicon substrate since they were not present in thicker films.

The spectrum collected from the Si 2p region of a nominal 50 Å thick film deposited at 417 °C is shown in Fig. 3. The peak shape consisted of one asymmetric peak and was consistent with elemental silicon from the substrate. No peaks were observed in the Si 2p spectrum to suggest silicon oxide or aluminum silicate. Therefore the observed oxygen and aluminum signals were collected from the entire film thickness and the oxygen was associated with the film, not an interfacial SiO $_x$  layer.

The atomic composition of nominal 50 Å thick films was determined by XPS and is displayed in Figs. 4 and 5. Each sample was sputter cleaned in the analysis chamber using Argon ion beam (500 eV Ar+, 300 nA/cm $^2$ , angle of incidence of 55° off sample normal) to remove adventitious hydrocarbons. Spectra

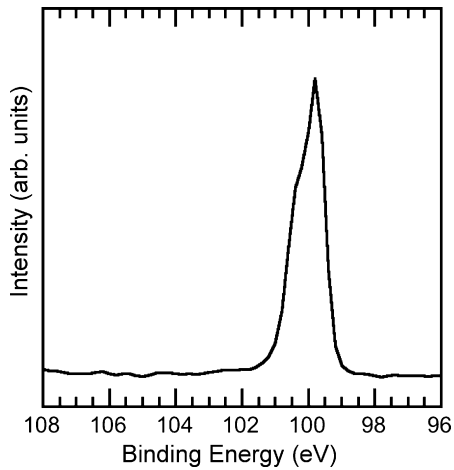


Fig. 3. High-resolution XPS spectrum collected from Si 2p region of 50 Å thick aluminum oxide film deposited on H-terminated silicon substrate at 417 °C. Peak position suggests that silicon signals originated from silicon substrate and not oxide or silicate layer.

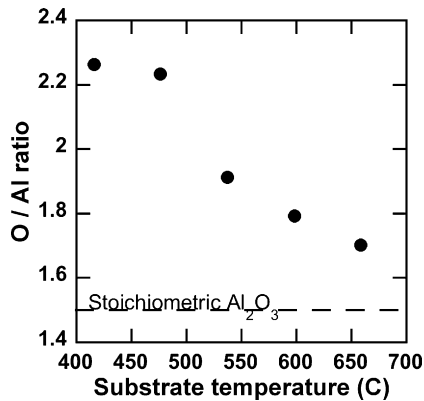


Fig. 4. Ratio of oxygen to aluminum atoms in films deposited from dimethylaluminum isopropoxide as determined by XPS analyses.

collected from the Al 2p and O 1s regions (not shown) contained peaks at positions consistent with aluminum oxide, and did not suggest that reduction occurred due to the ion beam cleaning. Peak areas were normalized using PHI sensitivity factors.<sup>12,13</sup>

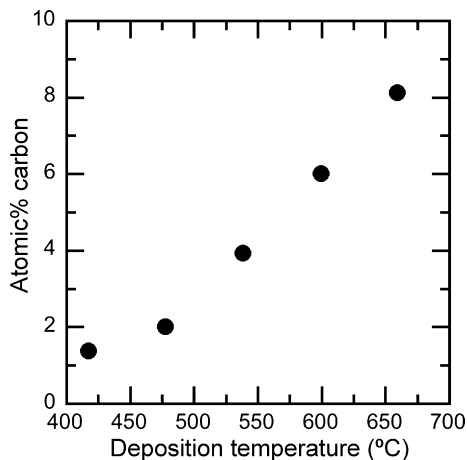


Fig. 5. Carbon content of films deposited from dimethylaluminum isopropoxide.

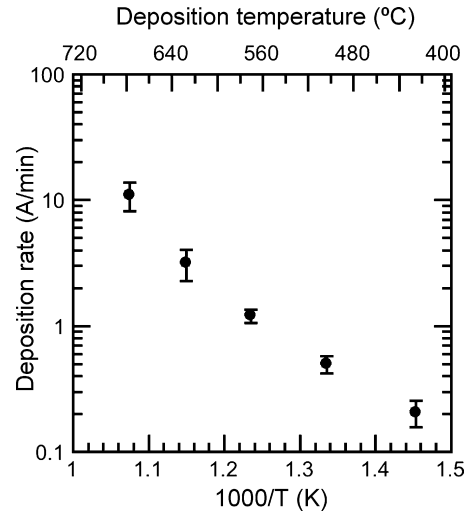


Fig. 6. Deposition rate of aluminum oxide films deposited from dimethylaluminum isopropoxide.

Two corrections were applied to the data prior to quantification: a correction to the sensitivity factors to account for the asymmetry of the photoionization process due to the geometry of the XPS system, and a correction to the measured peak area to account for the transmission characteristics of the analyzer optics.<sup>14</sup>

Oxygen to aluminum atom ratio in films is plotted as a function of deposition temperature in Fig. 4. At all deposition temperatures the oxygen to aluminum atom ratio was higher than that of stoichiometric  $\text{Al}_2\text{O}_3$ . Oxygen to aluminum atom ratio decreased with increasing deposition temperature. The trend of decreasing ratio with increasing deposition temperature is in agreement with reports of pyrolysis of AIP.<sup>15</sup>

Fig. 5 presents carbon concentration of deposited films as a function of deposition temperature. The carbon content increases from approximately 1.5 at.% to more than 8 at.% for films deposited at 417 and 659 °C, respectively. Films deposited from aluminum acetylacetonate precursors have been reported to exhibit a similar trend in carbon content with increasing deposition temperature. The carbon incorporation in the acetylacetonate-sourced alumina films approached 30 at.%, nearly 4 times that of our DMAI-sourced films.<sup>16,17</sup> Kobayashi reported an opposite trend in carbon incorporation as a function of deposition temperature in the deposition of alumina from the pyrolysis of AIP.<sup>18</sup>

### 3.2. Deposition kinetics

Fig. 6 plots film deposition rate of 17 samples versus reciprocal substrate temperature. Deposition rate is defined as the total film thickness at the wafer center, measured by *ex situ* spectroscopic ellipsometry, divided by the deposition time. Deposition time was defined as the elapsed time when the precursor bubbler was open. The plotted point at each temperature indicates the average deposition rate of all films deposited at that temperature. Error bars indicate the standard deviation of deposition rates at each temperature.

Deposition rates ranged from approximately 0.2 to 10 Å/min and the rate increased with increasing deposition temperature. Film growth was observed at all temperatures. This observation is in agreement with previous reports indicating that DMAI decomposition begins in the range 300–500 °C.<sup>7,15,19</sup> Deposition rate appeared linear with reciprocal temperature when plotted on a semi-logarithmic scale, and this suggested a kinetically controlled deposition mechanism under these process conditions. The reaction kinetics was assumed to follow an Arrhenius model, such that there is a linear relationship between the natural logarithm of the reaction rate (deposition rate, in this case) and the reciprocal reaction temperature (substrate temperature). A linear regression was fitted to the natural logarithm of deposition rate versus the reciprocal temperature ( $R^2 = 0.975$ ). The slope of the line is equal to the quantity ( $E_a/R$ ), where  $E_a$  is the apparent activation energy and  $R$  is the universal gas constant. An apparent activation energy of 86 kJ/mol was determined for this work. For comparison, the reported activation energy of film deposition from AIP with no co-reactant was reported to be 76 kJ/mol.<sup>20</sup>

#### 4. Conclusion

Chemical vapor deposition of aluminum oxide from dimethylaluminum isopropoxide as a function of deposition temperature was investigated. An effective activation energy for this process was determined to be 86 kJ/mol. Deposited films were shown to be oxygen-rich compared to Al<sub>2</sub>O<sub>3</sub>, with higher deposition temperatures resulting in films closer to stoichiometric alumina. Carbon content of the films increased from approximately 1 to 8 at.% at substrate temperatures of 417 and 659 °C, respectively. The production of Al<sub>2</sub>O<sub>3</sub> films from dimethylaluminum isopropoxide requires the removal of carbon atoms from the depositing film. The deposition rate increased with increased deposition temperature as shown in Fig. 5. This suggests that carbon in the precursor was trapped in the film as the deposition rate increased.

#### Acknowledgements

This work was funded by the Air Force Office of Scientific Research contract number FA9550-04-1-0448 and the National Science Foundation contract number DMR 0435843.

#### References

1. Haanappel VAC, van Corbach HD, Fransen T, Gellings PJ. *High Temperature Materials and Processes* 1994;**13**(2):149.
2. Jones AC, Aspinall HC, Chalker PR. *Surface & Coatings Technology* 2007;**201**(22–23):9046.
3. Bradley DC, Mehrotra RC, Gaur DP. *Metal alkoxides*. London: Academic Press; 1978.
4. Koh W, Ku S-J, Kim Y. *Thin Solid Films* 1997;**304**(1–2):222.
5. Barreca D, Battiston GA, Gerbasi R, Tondello E. *Journal of Materials Chemistry* 2000;**10**(9):2127.
6. Battiston GA, Gerbasi R. *Chemical Vapor Deposition* 2002;**8**(5):193.
7. Koo J, Kim S, Jeon S, Jeon H, Kim Y, Won Y. *Journal of the Korean Physical Society* 2006;**48**(1):131.
8. Mole T. *Australian Journal of Chemistry* 1966;**19**(3):373.
9. Rogers JH, Apblett AW, Cleaver WM, Tyler AN, Barron AR. *Journal of the Chemical Society, Dalton Transactions* 1992;**22**:3179.
10. Song Z, Sullivan LM, Rogers BR. *Journal of Vacuum Science & Technology A (Vacuum, Surfaces, and Films)* 2005;**23**(1):165.
11. Yablonovitch E, Allara DL, Chang CC, Gmitter T, Bright TB. *Physical Review Letters* 1986;**57**(2):249.
12. Stickle WF, Moulder JF, Sobol PE, Bomben KD. *Handbook of X-ray photoelectron spectroscopy*. Chanhassen, Minnesota: Physical Electronics USA, Inc.; 1995.
13. Ulvac-PHI, Inc. *Operator's PHI Multipak software manual, version 8.2C*. Chigasaki City, Kanagawa Prefecture, Japan: Ulvac-PHI, Inc.; 2007.
14. Fairley N, Carrick A. *The Casa cookbook, part 1: recipes for XPS data processing*. Cheshire, UK: Acolyte Science; 2005.
15. Lee SY, Luo B, Sun YM, White JM, Kim YS. *Applied Surface Science* 2004;**222**(1–4):234.
16. Singh MP, Raghavan G, Tyagi AK, Shivashankar SA. *Bulletin of Materials Science* 2002;**25**(2):163.
17. Temple D, Reisman A. *Journal of Electronic Materials* 1990;**19**(9):995.
18. Kobayashi T, Okamura M, Yamaguchi E, Shinoda Y, Hirota Y. *Journal of Applied Physics* 1981;**52**(10):6434.
19. An KS, Cho WT, Sung KH, Lee SS, Kim Y. *Bulletin of the Korean Chemical Society* 2003;**24**(11):1659.
20. Saraie J, Kown J, Yodogawa Y. *Journal of the Electrochemical Society* 1985;**132**(4):890.